This full text paper was peer reviewed at the direction of IEEE Communications Society subject matter experts for publication in the IEEE Globecom 2010 proceedings.

Channel-Matched Coding for Coarsely Quantized Coherent Optical Communication Systems

T. Lang*, A. Mezghani*, M. Kuschnerov†, B. Lankl† and J. A. Nossek*
* Technische Universität München, Arcisstr. 21, 80290 Munich, Germany. Email: Mezghani@nws.ei.tum.de
† Universität der Bundeswehr München, Werner-Heisenberg-Weg 39, 85577 Neubiberg, Germany.

***Abstract*—We present a channel-matched coding method for the compensation of dispersion in coarsely quantized coherent optical communication systems. The approach consists in optimizing a subset of equiprobable input symbols for each channel state, which is robust against dispersion and coarse quantization. This codebook optimization is solved efficiently using an iterative algorithm. The performance of the channel-matched codes is simulated for a 42.8Gbit/s dual-polarization coherent optical fiber system with QPSK modulation and single-bit analog-to-digital (A/D) conversion. Apart from the optimization, the proposed coding method does not increase the encoding/decoding complexity, but yields a considerable coding gain.**

I. Introduction

The performance of high-speed fiber optic links is limited by dispersion rather than only by noise [1]. Various electronic techniques have been proposed for the compensation of chromatic dispersion (CD) and polarization-mode dispersion (PMD). To our best knowledge, all existing approaches for electronic dispersion compensation use either precise ($\approx$ 3-6 bits) digital-to-analog converters (DACs) for electronic pre-equalization [2], or precise analog-to-digital converters (ADCs) for electronic post-equalization [3], [4]. Clearly, precise DACs and ADCs are one of the bottlenecks for very high transmission rates of 40Gbit/s and beyond.

Though, in a system with low-resolution (1-2 bits) DACs and ADCs conventional electronic equalization techniques are not applicable. Moreover, it was shown in [5] and [6] that standard (convolutional, LDPC) codes with small code rates or large block lengths would be necessary to communicate reliably over MIMO channels with single-bit ADCs.
In this paper, we present a channel-matched coding approach that takes the dispersion and coarse quantization fully into account and investigate its performance for a $4 \cdot 10.7$Gbit/s dual-polarization (DP) coherent optical fiber system with QPSK modulation and single-bit A/D conversion.

Notation: $(\bullet)^*$, $(\bullet)^{\mathrm{T}}$ and $(\bullet)^{\mathrm{H}}$ denote the conjugate, transpose and Hermitian transpose operators. Scalars, vectors and matrices are written in lower case, lower case bold and upper case bold italic letters, respectively. $[\boldsymbol{H}]_{i,j}$ denotes the (i,j)-th element of the matrix $\boldsymbol{H}$ and $[\boldsymbol{x}]_i$ is the i-th component of the vector $\boldsymbol{x}$. $a(t) \otimes b(t)$ is the convolution between the signals $a(t)$ and $b(t)$.

II. System Model

We consider a polarization-multiplexed coherent optical communication system. Two Mach-Zehnder modulators modulate the output of the laser with the pulse shaped input signals $x_1(t)$ and $x_2(t)$ using QPSK. The orthogonally polarized signals are combined and passed through a standard single-mode fiber (SMF). The received signal is optically filtered (Gauss, 2nd order, 35GHz bandwidth), split into two paths, mixed down with a local oscillator using a network of two 90° hybrids and coherently detected by four balanced photodetectors. The in-phase and quadrature-phase baseband signals are electrically filtered (Bessel, 5th order, optimized bandwidth which minimizes the pulse spreading), sampled at the symbol rate $f_s = 1/T_s$ and 1-bit A/D converted (separate quantization of real and imaginary parts).

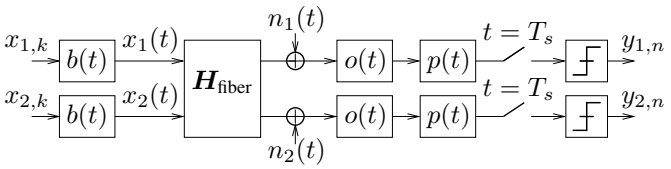

Figure 1. Baseband model of the dual-polarization coherent optical fiber system with QPSK modulation and single-bit outputs.

Fig. 1 depicts the equivalent baseband model. The k-th input symbol for the j-th polarization-mode $x_{j,k}$ is linearly convolved with the pulse shape signal $b(t)$, the channel impulse responses $h_{ij}(t)$ (i-th output polarization, j-th input polarization), the optical filter $o(t)$ and the electrical filter $p(t)$. Thus, the n-th quantized channel output of the i-th polarization-mode at sample time nT_s is given by

$$y_{i,n} = \mathcal{Q}\left\{ \sum_{k=-\infty}^{\infty} \sum_{j=1}^{2} x_{j,n-k} q_{ij}(kT_s) + \eta_{i,n} \right\} \in \{\pm 1 \pm \mathrm{j}\}, \quad (1)$$

where $q_{ij}(t) = b(t) \otimes h_{ij}(t) \otimes o(t) \otimes p(t)$ and $\eta_{i,n} = \eta_i(nT_s) = n(t) \otimes o(t) \otimes p(t)$. The quantization operator $\mathcal{Q}\{\bullet\}$ evaluates the sign of the imaginary and real part of its argument, i.e., $\mathcal{Q}\{\bullet\} = \mathrm{sign}(\Re\{\bullet\}) + \mathrm{j} \cdot \mathrm{sign}(\Im\{\bullet\})$. The QPSK input symbols are normalized to one, that is $x_{j,n-k} \in \{(\pm 1 \pm \mathrm{j})/\sqrt{2}\}$.

The sampled noise $\eta_{i,n}$ is assumed to be additive white Gaussian with variance $\sigma_\eta^2 = N_0 f_s$, where N_0 is the two-sided noise power spectral density. Given that the CD and PMD spreads the input impulses over $L+1$ sample intervals, (1) can be expressed in vector notation as

$$\boldsymbol{y}_n = \mathcal{Q}\left\{ \sum\nolimits_{k=0}^{L} \boldsymbol{H}_k \boldsymbol{x}_{n-k} + \boldsymbol{\eta}_n \right\}. \quad (2)$$

978-1-4244-5638-3/10/$26.00 ©2010 IEEE

Here, $[\boldsymbol{H}_k]_{ij} = q_{ij}(kT_s)$, $\boldsymbol{x}_{n-k} = [x_{1,n-k}, x_{2,n-k}]^{\mathrm{T}}$, $\boldsymbol{y}_n = [y_{1,n}, y_{2,n}]^{\mathrm{T}}$ and $\boldsymbol{\eta}_n = [\eta_{1,n}, \eta_{2,n}]^{\mathrm{T}}$ with diagonal covariance matrix $\mathrm{E}[\boldsymbol{\eta}_n \boldsymbol{\eta}_n^{\mathrm{H}}] = \sigma_\eta^2 \mathbf{I}_2$.

Clearly, this channel is an example of a finite-state intersymbol-interference (ISI) channel with input $\boldsymbol{x}_n \in \mathcal{X} = \{(\pm 1 \pm \mathrm{j})/\sqrt{2}\}^2$, output $\boldsymbol{y}_n \in \mathcal{Y} = \{\pm 1 \pm \mathrm{j}\}^2$ and channel transition probabilities $\Pr(\boldsymbol{y}_n | \boldsymbol{x}_{n-L}, \boldsymbol{x}_{n-L+1}, \ldots, \boldsymbol{x}_n)$.

The optical signal-to-noise ratio (OSNR) is defined by

$$\mathrm{OSNR}[\mathrm{dB}] = \mathrm{SNR}[\mathrm{dB}] + 10 \cdot \log_{10}(f_s/12.5\mathrm{GHz}), \quad (3)$$

where $\mathrm{SNR} = 1/\sigma_\eta^2$. Based on a commonly used model for the PMD and CD the Fourier transform of the dually polarized channel $\boldsymbol{H}_{\text{fiber}}(\omega = 2\pi f) = \mathcal{F}(\boldsymbol{h}_{\text{fiber}}(t))$ with $h_{ij}(t) = [\boldsymbol{h}_{\text{fiber}}(t)]_{ij}$ is given by

$$\boldsymbol{H}_{\text{fiber}}(2\pi f) = \begin{bmatrix} \cos(\theta) & -\sin(\theta) \\ \sin(\theta) & \cos(\theta) \end{bmatrix} \begin{bmatrix} e^{j\alpha} & 0 \\ 0 & e^{-j\alpha} \end{bmatrix} \times \begin{bmatrix} \cos(\theta) & \sin(\theta) \\ -\sin(\theta) & \cos(\theta) \end{bmatrix} e^{-j\pi \frac{\lambda_0^2}{c} D L_{\text{fiber}} f^2}. \quad (4)$$

Here, $\alpha = (2\pi f \tau + \phi/2)$, $D = 16.8$ps/nm/km is the dispersion parameter at wavelength $\lambda_0 = 1550$nm, c is the speed of light, L_{fiber} is the length of the uncompensated fiber, $f = f_s$ is the baseband frequency, τ is the instantaneous differential group delay (DGD) between the polarization-modes and the term $H_{\text{CD}}(f) = e^{-j\pi\lambda_0^2 D L_{\text{fiber}} f^2/c}$ accounts for the fiber's CD. The phase ϕ and angle θ are random and uniformly distributed in the interval $[0;2\pi]$. In this work, we focus on CD and PMD and neglect the dispersion slope, the polarization-dependent loss as well as the nonlinear Kerr effect. Finally, we assume that only CD contributes significantly to ISI and ignore the DGD, i.e., $\tau = 0$. Fig. 2 shows the magnitude of the impulse response of the fiber's CD for different symbol rates f_s and a dispersion of 1000ps/nm. Clearly, higher symbol rates lead to stronger distortion and ISI.

It is worth noting, that the proposed channel-matched coding method is not restricted to this specific channel model. In fact, the codebook optimizations in Sections III and IV are solely based on the channel transition probabilities, which can be estimated for any (nonlinear) channel with finite input and output alphabets. Nevertheless, the application of channel-matched coding requires that the receiver (transmitter) has access to the channel state information (CSI), optimizes the codebook and feeds its choice back to the transmitter (receiver). Moreover, the channel has to be slowly time-varying, which is the case in optical communication systems.

III. Design of Channel-Matched Block Codes

Channel-matched block codes of length W are defined as a subset $\mathcal{S} \subseteq \mathcal{X}^W$ of 2^K equiprobable input vector sequences $\boldsymbol{x}_{n-W+1}^n = [\boldsymbol{x}_{n-W+1}, \ldots, \boldsymbol{x}_n]$ of length W, that is

$$\Pr(\boldsymbol{x}_{n-W+1}^n) = \begin{cases} 2^{-K} & \text{for } \boldsymbol{x}_{n-W+1}^n \in \mathcal{S} \subseteq \mathcal{X}^W \\ 0 & \text{otherwise} \end{cases}. \quad (5)$$

According to (5) K source bits can be mapped directly to one of the selected input sequences $\boldsymbol{x}_{n-W+1}^n \in \mathcal{S}$. The code rate equals $R = \log_2(|\mathcal{S}|)/\log_2(|\mathcal{X}|^W) = K/(4W)$. A channel-matched block code can partially remove the ISI by considering the mutual influence between the simultaneously encoded input vectors $[\boldsymbol{x}_{n-W+1}, \ldots, \boldsymbol{x}_n]$. The following equation with $L+1 = 3$ channel taps and block length of $W = 2$ illustrates the influence that $\boldsymbol{x}_{n-1}$ exerts on $\boldsymbol{x}_n$ and vice versa

$$\boldsymbol{y}_n^{n+1} = \mathcal{Q}\{[\boldsymbol{H}_0\boldsymbol{x}_n + \boldsymbol{H}_1\boldsymbol{x}_{n-1} + \boldsymbol{H}_2\boldsymbol{x}_{n-2} + \boldsymbol{\eta}_n\ , \boldsymbol{H}_0\boldsymbol{x}_{n+1} + \boldsymbol{H}_1\boldsymbol{x}_n + \boldsymbol{H}_2\boldsymbol{x}_{n-1} + \boldsymbol{\eta}_{n+1}]\}. \quad (6)$$

The symbols $\boldsymbol{x}_{n-2}$ and $\boldsymbol{x}_{n+1}$ interfere with $\boldsymbol{x}_{n-1}^n$ and thus distort the channel output sequence $\boldsymbol{y}_n^{n+1} = [\boldsymbol{y}_n, \boldsymbol{y}_{n+1}]$. Though, due to (5) the encoder can not take this interference into account. Our approach is to model the unknown interference caused by the k-th channel tap as additional AWGN with diagonal covariance matrix $\mathrm{E}[\boldsymbol{\rho}_k \boldsymbol{\rho}_k^{\mathrm{H}}] = \mathrm{diag}(\rho_{k1}^2, \rho_{k2}^2)$ and

$$\rho_{ki}^2 = \mathrm{Var}\left[\left\{\left(\sum\nolimits_{j=1}^{2} [\boldsymbol{H}_k]_{i,j} [\boldsymbol{x}_{n-k}]_j\right) : \boldsymbol{x}_{n-k} \in \mathcal{X}\right\}\right].$$

Fig. 2 shows that most of the transmit energy is conveyed over the middle channel tap. This property can be exploited for an approximation of (6), that is

$$\boldsymbol{y}_n^{n+1} \approx \mathcal{Q}\{[\boldsymbol{H}_0\boldsymbol{x}_n + \boldsymbol{H}_1\boldsymbol{x}_{n-1} + \boldsymbol{\rho}_2 + \boldsymbol{\eta}_n\ , \boldsymbol{H}_1\boldsymbol{x}_n + \boldsymbol{H}_2\boldsymbol{x}_{n-1} + \boldsymbol{\rho}_0 + \boldsymbol{\eta}_{n+1}]\}. \quad (7)$$

In fact, (7) defines a discrete memoryless channel (DMC) with input $\boldsymbol{x}_{n-1}^n \in \mathcal{X}^2$, output $\boldsymbol{y}_n^{n+1} \in \mathcal{Y}^2$ and transition probabilities

$$\Pr(\boldsymbol{y}_n^{n+1} | \boldsymbol{x}_{n-1}^n) = \prod_{c \in \{\mathbb{R},\mathbb{I}\}} \prod_{i=1}^{2} \Phi\left(\frac{[\boldsymbol{y}_n]_{c,i} [\sum_{k=0}^{1} \boldsymbol{H}_k \boldsymbol{x}_{n-k}]_{c,i}}{\sqrt{(\sigma_\eta^2 + \rho_{2i}^2)/2}}\right) \times \prod_{j=1}^{2} \Phi\left(\frac{[\boldsymbol{y}_{n+1}]_{c,j} [\boldsymbol{H}_1\boldsymbol{x}_n + \boldsymbol{H}_2\boldsymbol{x}_{n-1}]_{c,j}}{\sqrt{(\sigma_\eta^2 + \rho_{0j}^2)/2}}\right). \quad (8)$$

Here, the cumulative normal distribution function $\Phi(x) = \frac{1}{\sqrt{2\pi}} \int_{-\infty}^{x} e^{-\frac{t^2}{2}} dt$ is evaluated separately for real parts $c = \mathbb{R}$ and imaginary parts $c = \mathbb{I}$.

Now, the codebook optimization approach in [5], [6] is applied to generate a channel-matched block code that is robust against ISI and coarse quantization. In particular, we

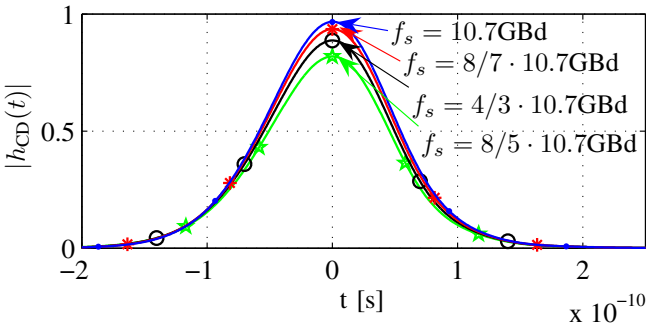

Figure 2. Impulse response of the fiber's CD for different symbol rates f_s and a dispersion of 1000ps/nm.

Algorithm 1 Iterative Capacity Maximization (C-max)

1: **initialization** $\mathcal{S} = \mathcal{X}^2$, $L_{\boldsymbol{y}|\boldsymbol{x}} = \log_2(\Pr(\boldsymbol{y}|\boldsymbol{x}))$
2: **while** $|\mathcal{S}| > 2^K$ **do**
3: **for all** $\boldsymbol{y} \in \mathcal{Y}$ **do**
4: $L_{\boldsymbol{y}} = \log_2\left(\sum_{\boldsymbol{x}\in\mathcal{S}} \Pr(\boldsymbol{y}|\boldsymbol{x})\right)$
5: **for all** $\boldsymbol{x} \in \mathcal{S}$ **do**
6: $\alpha_{\boldsymbol{x}} = \sum_{\boldsymbol{y}\in\mathcal{Y}} \Pr(\boldsymbol{y}|\boldsymbol{x}) \cdot (L_{\boldsymbol{y}|\boldsymbol{x}} - L_{\boldsymbol{y}})$
7: $\boldsymbol{z} = \arg\min_{\boldsymbol{x}\in\mathcal{S}}\{\alpha_{\boldsymbol{x}}\}$ and $\mathcal{S} \leftarrow \mathcal{S} \setminus \boldsymbol{z}$

try to find a subset $\mathcal{S} \subseteq \mathcal{X}^2$ of input sequences $\boldsymbol{x}_{n-1}^n \in \mathcal{X}^2$ that maximizes the mutual information between the input and output of the DMC, that is

$$\begin{aligned}\max_{\mathcal{S}\subseteq\mathcal{X}^2} I(X;Y) &= \max_{\mathcal{S}\subseteq\mathcal{X}^2}\left\{-H(\boldsymbol{y}_n^{n+1}|\boldsymbol{x}_{n-1}^n)\right\} \\ &= \max_{\mathcal{S}\subseteq\mathcal{X}^2}\left\{\sum_{\boldsymbol{y}_n^{n+1}\in\mathcal{Y}^2}\sum_{\boldsymbol{x}_{n-1}^n\in\mathcal{S}} \Pr(\boldsymbol{y}_n^{n+1}|\boldsymbol{x}_{n-1}^n)\right. \\ &\quad \left.\times \log_2\left(\frac{\Pr(\boldsymbol{y}_n^{n+1}|x_{n-1}^n)}{\sum_{\tilde{\boldsymbol{x}}_{n-1}^n\in\mathcal{S}}\Pr(\boldsymbol{y}_n^{n+1}|\tilde{\boldsymbol{x}}_{n-1}^n)}\right)\right\} \quad (9) \\ &= \max_{\mathcal{S}\subseteq\mathcal{X}^2}\left\{\sum_{\boldsymbol{x}_{n-1}^n\in\mathcal{S}} \alpha_{\boldsymbol{x}_{n-1}^n}\right\}, \quad (10)\end{aligned}$$

where $H(\boldsymbol{y}_n^{n+1}|\boldsymbol{x}_{n-1}^n)$ is the conditional entropy.

The optimization problem in (10) can be solved suboptimally by means of the *iterative capacity maximization* (C-max) algorithm proposed in [6], which exhibits a rather low complexity for the given alphabet sizes $|\mathcal{X}|^2 = |\mathcal{Y}|^2 = 256$. The C-max algorithm, which constitutes a suboptimal iterative solution to (10), is summarized in Algorithm 1 (the indices n and $n-1$ are omitted for simplicity). In each iteration the C-max algorithm evaluates the (negative) contribution $\alpha_{\boldsymbol{x}}$ of each individual $\boldsymbol{x} \in \mathcal{S}$ to the mutual information. Subsequently, the input symbol with the smallest $\alpha_{\boldsymbol{x}}$ is removed from the set of remaining input symbols in line 7. After $(|\mathcal{X}^2| - 2^K)$ iterations, the algorithm delivers the optimized symbol selection $\mathcal{S}$. The result of the C-max algorithm can be improved posteriorly by another algorithm presented in [6] and called *binary symbol switching* (BSS), which is based on a systematic symbol switching, i.e., replacing "bad" symbols of $\mathcal{S}$ by others from $\mathcal{X}^2 \setminus \mathcal{S}$ (see [6] for more details).

IV. Design of Channel-Matched Codes with Memory

Channel-matched codes of length W and memory depth M are defined as a collection of $|\mathcal{X}|^M$ channel-matched block codes $\mathcal{S}_1, \mathcal{S}_2, \ldots, \mathcal{S}_{|\mathcal{X}|^M}$ each of which is optimized for a specific channel state $\boldsymbol{x}_{n-W+1-M}^{n-W} \in \mathcal{X}^M$. Hence, the codebook $\mathcal{S}_i$ for the i-th channel state $\xi_i = \boldsymbol{x}_{n-W+1-M}^{n-W}$ is defined by the conditional input distribution

$$\Pr(\boldsymbol{x}_{n-W+1}^n|\xi_i) = \begin{cases} 2^{-K} & \text{for } \boldsymbol{x}_{n-W+1}^n \in \mathcal{S}_i \subseteq \mathcal{X}^W \\ 0 & \text{otherwise}\end{cases}. \quad (11)$$

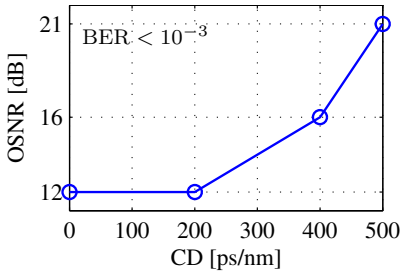

Figure 3. Direct detection of channel-matched block codes of length $M = 2$ and code rate $R = 1/2$. Average result for 1000 random channels.

Every codebook contains an optimized selection of $|\mathcal{S}_i| = 2^K$ input vector sequences and the rate of the code equals $R = K/(4W)$. In contrast to (5), the interference caused by the previous M input vectors $\boldsymbol{x}_{n-W+1-M}^{n-W} \in \mathcal{X}^M$ is taken into account by the encoding rule in (11). Accordingly, a channel-matched code of length $W = 2$ and memory depth $M = 1$ allows us to approximate (6) pursuant to

$$\begin{aligned}\boldsymbol{y}_n^{n+1} \approx \mathcal{Q}\{[&\boldsymbol{H}_0\boldsymbol{x}_n + \boldsymbol{H}_1\boldsymbol{x}_{n-1} + \boldsymbol{H}_2\boldsymbol{x}_{n-2} + \boldsymbol{\eta}_n\ , \\ &\boldsymbol{H}_1\boldsymbol{x}_n + \boldsymbol{H}_2\boldsymbol{x}_{n-1} + \boldsymbol{\rho}_0 + \boldsymbol{\eta}_{n+1}]\}. \quad (12)\end{aligned}$$

Thereby, each channel state $\xi_i = \boldsymbol{x}_{n-2} \in \mathcal{X}$ in (12) defines a DMC with input $\boldsymbol{x}_{n-2}^n = [\xi_i, \boldsymbol{x}_{n-1}^n]$, output $\boldsymbol{y}_n^{n+1}$ and transition probabilities

$$\begin{aligned}\Pr(\boldsymbol{y}_n^{n+1}|\boldsymbol{x}_{n-2}^n) = &\prod_{c\in\{\mathbb{R},\mathbb{I}\}}\prod_{i=1}^{2}\Phi\left(\frac{[\boldsymbol{y}_n]_{c,i}[\sum_{k=0}^{2}\boldsymbol{H}_k\boldsymbol{x}_{n-k}]_{c,i}}{\sigma_\eta/\sqrt{2}}\right) \\ &\times\prod_{j=1}^{2}\Phi\left(\frac{[\boldsymbol{y}_{n+1}]_{c,j}[\boldsymbol{H}_1\boldsymbol{x}_n + \boldsymbol{H}_2\boldsymbol{x}_{n-1}]_{c,j}}{\sqrt{(\sigma_\eta^2+\rho_{0j}^2)/2}}\right). \quad (13)\end{aligned}$$

The C-max BSS algorithm discussed above can be used to optimize a channel-matched block code for each possible ξ_i. Thus, for $M = 1$, we obtain a collection of 16 codebooks $\mathcal{S}_1, \mathcal{S}_2, \ldots, \mathcal{S}_{16}$. Other more sophisticated methods but computationally intensive for optimizing the channel-matched memory code are presented in [7], which can be also used to evaluate the Shannon-capacity of the optical system.

V. Simulation Results

Let us consider a DP coherent optical fiber system with QPSK modulation and single-bit outputs (as defined in Section II) at a net data rate of $4 \cdot 10.7$Gbit/s. The coding overhead is compensated by increasing the symbol rate appropriately, i.e., $f_s \cdot R = \text{const}$. As Fig. 2 illustrates, strong (low rate) codes are affected by a stronger ISI.

Fig. 3 shows that the channel-matched block codes of Section III combined with simple direct detection can compensate a CD of up to 500ps/nm, which corresponds to a channel with $L + 1 = 3$ dominant taps. Direct detection means that the maximum-likelihood estimate is only based on a small output sequence of length 2, i.e.,

$$\hat{\boldsymbol{x}}_{n-1}^n = \arg\max_{\boldsymbol{x}_{n-1}^n\in\mathcal{S}}\{\Pr(\boldsymbol{y}_n^{n+1}|\boldsymbol{x}_{n-1}^n)\}. \quad (14)$$

978-1-4244-5638-3/10/$26.00 ©2010 IEEE

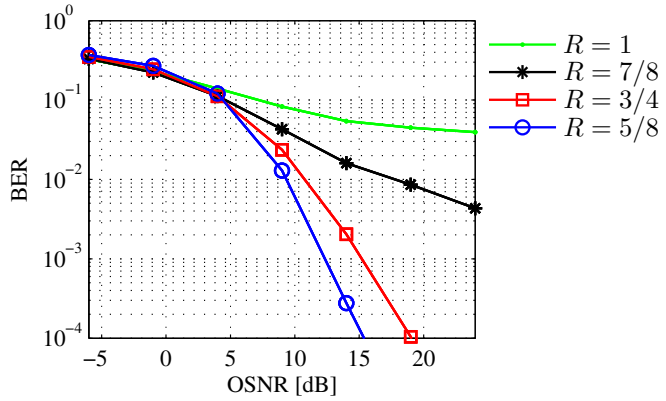

Figure 4. MAP decoding of channel-matched codes with block length $W = 2$, memory depth $M = 1$ and different code rates. Average of 3 random channels with 500ps/nm CD and $4 \cdot 10.7$Gbit/s net data rate.

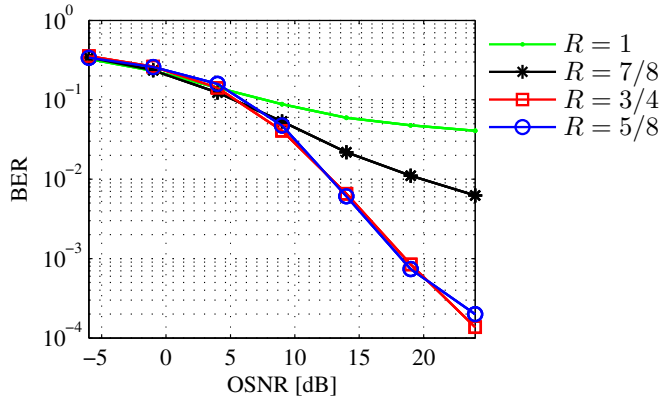

Figure 5. MAP decoding of channel-matched codes with block length $W = 2$, memory depth $M = 1$ and different code rates. Average of 3 random channels with 1000ps/nm CD and $4 \cdot 10.7$Gbit/s net data rate.

As the size of the output alphabet is finite, all possible ML estimates can be computed in advance and stored in a look-up table with $|\mathcal{Y}|^2 = 256$ entries. In Fig. 4 and Fig. 5 we performed MAP decoding for three random channels with a CD of 500ps/nm and 1000ps/nm, respectively. Thereby, we employed a BCJR decoder [8] with memory $W = 2$, which operates on a trellis with $|\mathcal{X}|^2 = 256$ states and $|\mathcal{X}|^2 \cdot 2^{R \cdot \log_2(|\mathcal{X}|^2)} = 256 \cdot 2^K$ transitions between the states. However, there are 5 non-zero taps at a CD of 1000ps/nm for $f_s \geq 4/3 \cdot 10.7$GBd or rather $R \leq 3/4$ as can be seen from Fig. 2. Fig. 5 shows that the channel-matched codes of Section IV with $W = 2$ and $M = 1$ can compensate a CD of up to 1000ps/nm. Moreover, Fig. 4 and Fig. 5 demonstrate that strong codes with $R \leq 3/4$ lead to better results than high rate codes, even though the channel is operated at a higher symbol rate f_s.

Most importantly, channel-matched coding leads to a considerable gain compared to the uncoded case ($R = 1$). Furthermore, apart from the codebook optimization, channel-matched coding does not increase the encoding/decoding complexity. In fact, channel-matched block codes even reduce the number of valid transitions in the decoding trellis.

VI. Conclusion

We propose the application of channel-matched codes to replace pre- or post-equalizers, which rely on high resolution DACs or ADCs [3]. In particular, we investigated a DP coherent optical fiber system with QPSK modulation and single-bit A/D conversion at a net data rate of 42.8Gbit/s. The channel-matched coding method works directly with channel transition probabilities, which can be estimated for any (nonlinear) channel with finite input and output alphabets. The complexity for the codebook optimization is kept low by decomposing and approximating the finite-state ISI channel with a set of DMCs. For each of these DMCs an optimized codebook is computed efficiently using an iterative algorithm. The resulting channel-matched code is robust against coarse quantization, PMD and a CD of up to 1000ps/nm. Moreover, simple direct detection of optimized channel-matched block codes is feasible at a CD of 500ps/nm.

References

[1] A. C. Singer, N. R. Shanbhag, and H.-M. Bae, "Electronic Dispersion Compensation," *IEEE Signal Processing Magazine*, vol. 25, no. 6, pp. 110–130, Nov. 2008.

[2] R. Waegemans, S. Herbst, L. Holbein, P. Watts, P. Bayvel, C. Fürst, and R. I. Killey, "10.7 Gb/s electronic predistortion transmitter using commercial FPGAs and D/A converters implementing real-time DSP for chromatic dispersion and SPM compensation," *Optics Express,*, vol. 17, no. 10, pp. 8630–8640, 2009.

[3] H. Sun, K.-T. Wu, and K. Roberts, "Real-time measurements of a 40 Gb/s coherent system," *Optics Express*, vol. 16, no. 2, pp. 873–879, 2008.

[4] T. Pfau, S. Hoffmann, O. Adamczyk, R. Peveling, V. Herath, M. Porrmann, and Reinhold Noé, "Coherent optical communication: Towards realtime systems at 40 Gbit/s and beyond," *Optics Express*, vol. 16, no. 2, pp. 866–872, 2008.

[5] A. Mezghani, M. T. Ivrlac, and J. A. Nossek, "Achieving near-Capacity on Large Discrete Memoryless Channels with Uniform Distributed Selected Input," *International Symposium on Information Theory and its Applications (ISITA)*, Dec. 2008.

[6] T. Lang, A. Mezghani, and J. A. Nossek, "Channel-Adaptive Coding for Coarsely Quantized MIMO Systems," in *International Workshop on Signal Processing Advances for Wireless Communications*, Feb. 23–24, 2010.

[7] T. Lang, A. Mezghani, and J. A. Nossek, "Channel-Matched trellis Codes for Finite-State Intersymbol-Interference Channels," in *International ITG Workshop on Smart Antennas*, Feb. 23–24, 2010.

[8] L. Bahl, J. Cocke, F. Jelinek, and J. Raviv, "Optimal Decoding of Linear Codes for Minimizing Symbol Error Rate (corresp.)," *IEEE Transactions on Information Theory*, vol. 20, pp. 284–287, Mar. 1974.

978-1-4244-5638-3/10/$26.00 ©2010 IEEE